

1 A content-sensitive framework for modeling episodic
2 memory reveals event-like structure in naturalistic
3 experience, recall, and neural processing

4 Andrew C. Heusser, Paxton C. Fitzpatrick, and Jeremy R. Manning

5 Department of Psychological and Brain Sciences

6 Dartmouth College, Hanover, NH 03755, USA

7 Corresponding author: jeremy.r.manning@dartmouth.edu

8 August 30, 2019

9 **Abstract**

10 Our life experiences unfold over time in highly complex manner, with the evolving presence
11 of numerous intricate features describing our journey between each event we encounter. Here,
12 we propose a framework for mapping dynamic naturalistic episodes onto geometric spaces as
13 *experience trajectories* that capture the temporal dynamics of real-world content. Within this
14 geometric framework, one may compare the shape of the trajectory formed by an experience to
15 that defined by one's later recollection to characterize our memories' recovery and distortion of
16 the external world. Here, we apply this approach to a naturalistic memory experiment in which
17 participants viewed and verbally recounted a video, and find that the video and subsequent
18 recalls share both an experience-specific shape and a discernible event-like structure. Despite
19 this apparent similarity, we find that the level of *precision* with which individuals recounted
various events and the *distinctiveness* of recall for those events were varied and predictive of
overall memory performance. Finally, we identify a network of brain structures that is sensitive
to the "shapes" of our ongoing experiences, and an overlapping network sensitive to how we will

20 later remember them. Our framework and findings underscore the rich event-like structure of
21 the external world and our memories, and offer novel, content-sensitive measures for assessing
22 episodic memory

23 **Introduction**

24 What does it mean to *remember* something? In traditional episodic memory experiments (e.g.,
25 list-learning or trial-based experiments; Murdock, 1962; Kahana, 1996), remembering is often cast
26 as a discrete and binary operation: each studied item may be separated from all others, and la-
beled as having been recalled or forgotten. More nuanced studies might incorporate self-reported
27 confidence measures as a proxy for memory strength, or ask participants to discriminate between
28 “recollecting” the (contextual) details of an experience or having a general feeling of “familiarity”
29 (Yonelinas, 2002). Using well-controlled, trial-based experimental designs, the field has amassed
30 a wealth of valuable information regarding human episodic memory. However, there are funda-
31 mental properties of the external world and our memories that trial-based experiments are not well
32 suited to capture (for review also see Koriat and Goldsmith, 1994; Huk et al., 2018). First, our expe-
33 riences and memories are continuous, rather than discrete—removing a (naturalistic) event from
34 the context in which it occurs can substantially change its meaning. Second, the specific language
35 used to describe an experience has little bearing on whether the experience should be considered to
36 have been “remembered.” Asking whether the rememberer has precisely reproduced a specific set
37 of words to describe a given experience is nearly orthogonal to whether they were actually able to
38 remember it. In classic (e.g., list-learning) memory studies, by contrast, the number or proportion
39 of precise recalls is often a primary metric for assessing the quality of participants’ memories.
40 Third, one might remember the *essence* (or a general summary) of an experience but forget (or
41 neglect to recount) particular details. Capturing the essence of what happened is typically the
42 main “point” of recounting a memory to a listener, while the addition of highly specific details
43 may add comparatively little to successful conveyance of an experience.

45 How might one go about formally characterizing the “essence” of an experience, or whether

46 it has been recovered by the rememberer? Any given moment of an experience derives meaning
47 from surrounding moments, as well as from longer-range temporal associations (Lerner et al.,
48 2011; Manning, 2019). Therefore, the timecourse describing how an event unfolds is fundamental
49 to its overall meaning. Further, this hierarchy formed by our subjective experiences at different
50 timescales defines a *context* for each new moment (e.g., Howard and Kahana, 2002; Howard et al.,
51 2014), and plays an important role in how we interpret that moment and remember it later (for
52 review see Manning et al., 2015). Our memory systems can leverage these associations to form
53 predictions that help guide our behaviors (Ranganath and Ritchey, 2012). For example, as we
54 navigate the world, the features of our subjective experiences tend to change gradually (e.g., the
55 room or situation we are in at any given moment is strongly temporally autocorrelated), allowing
56 us to form stable estimates of our current situation and behave accordingly (Zacks et al., 2007;
57 Zwaan and Radvansky, 1998).

58 Although our experiences most often change gradually, they also occasionally change sud-
59 denly (e.g., when we walk through a doorway; Radvansky and Zacks, 2017). Prior research
60 suggests that these sharp transitions (termed *event boundaries*) during an experience help to dis-
61 cretize our experiences (and their mental representations) into *events* (Radvansky and Zacks, 2017;
62 Brunec et al., 2018; Heusser et al., 2018a; Clewett and Davachi, 2017; Ezzyat and Davachi, 2011;
63 DuBrow and Davachi, 2013). The interplay between the stable (within event) and transient (across
64 event) temporal dynamics of an experience also provides a potential framework for transforming
65 experiences into memories that distill those experiences down to their essence. For example, prior
66 work has shown that event boundaries can influence how we learn sequences of items (Heusser
67 et al., 2018a; DuBrow and Davachi, 2013), navigate (Brunec et al., 2018), and remember and un-
68 derstand narratives (Zwaan and Radvansky, 1998; Ezzyat and Davachi, 2011). Prior research has
69 implicated the hippocampus and the medial prefrontal cortex as playing a critical role in trans-
70 forming experiences into structured and consolidated memories (Tompry and Davachi, 2017).

71 Here we sought to examine how the temporal dynamics of a “naturalistic” experience were
72 later reflected in participants’ memories. We analyzed an open dataset that comprised behavioral
73 and functional Magnetic Resonance Imaging (fMRI) data collected as participants viewed and then

74 verbally recounted an episode of the BBC television series *Sherlock* (Chen et al., 2017). We developed
75 a computational framework for characterizing the temporal dynamics of the moment-by-moment
76 content of the episode and of participants' verbal recalls. Specifically, we use topic modeling (Blei
77 et al., 2003) to characterize the thematic conceptual (semantic) content present in each moment of
78 the episode and recalls, and Hidden Markov Models (Rabiner, 1989; Baldassano et al., 2017) to
79 discretize this evolving semantic content into events. In this way, we cast naturalistic experiences
80 (and recalls of those experiences) as *trajectories* that describe how the experiences evolve over
81 time. Under this framework, successful remembering entails verbally "traversing" the content
82 trajectory of the episode, thereby reproducing the shape (or essence) of the original experience.
83 Comparing the shapes of the topic trajectories of the episode and of participants' retellings of the
84 episode then reveals which aspects of the episode were preserved (or lost) in the translation into
85 memory. We further examine whether 1) the *precision* with which a participant recounts each event
86 and 2) the *distinctiveness* each recall event is (relative to the other recalled events) relates to their
87 overall memory performance. Last, we identify networks of brain structures whose responses
88 (as participants watched the episode) reflected the temporal dynamics of the episode, and how
89 participants would later recount the episode.

90 Results

91 To characterize the shape of the *Sherlock* episode and participants' subsequent recounts of its
92 unfolding, we used a topic model (Blei et al., 2003) to discover the latent themes in the episode's
93 dynamic content. Topic models take as inputs a vocabulary of words to consider and a collection
94 of text documents, and return two output matrices. The first of these is a *topics matrix* whose rows
95 are topics (latent themes) and whose columns correspond to words in the vocabulary. The entries
96 of the topics matrix define how each word in the vocabulary is weighted by each discovered topic.
97 For example, a detective-themed topic might weight heavily on words like "crime," and "search."
98 The second output is a *topic proportions matrix*, with one row per document and one column per
99 topic. The topic proportions matrix describes what mixture of discovered topics is reflected in each

100 document.

101 Chen et al. (2017) collected hand-annotated information about each of 1000 (manually identified)
102 scenes spanning the roughly 50 minute video used in their experiment. This information included:
103 a brief narrative description of what was happening; whether the scene took place indoors or
104 outdoors; the names of any characters on the screen; the names of any characters who were in
105 focus in the camera shot; the names of characters who were speaking; the location where the scene
106 took place; the camera angle (close up, medium, long, etc.); whether or not background music was
107 present; and other similar details (for a full list of annotated features see *Methods*). We took from
108 these annotations the union of all unique words (excluding stop words, such as “and,” “or,” “but,”
109 etc.) across all features and scenes as the “vocabulary” for the topic model. We then concatenated
110 the sets of words across all features contained in overlapping, 50-scene sliding windows, and
111 treated each 50-scene sequence as a single “document” for the purpose of fitting the topic model.
112 Next, we fit a topic model with (up to) $K = 100$ topics to this collection of documents. We found that
113 27 unique topics (with non-zero weights) were sufficient to describe the time-varying content of the
114 video (see *Methods*; Figs. 1, S2). Note that our approach is similar in some respects to Dynamic Topic
115 Models (Blei and Lafferty, 2006) in that we sought to characterize how the thematic content of the
116 episode evolved over time. However, whereas Dynamic Topic Models are designed to characterize
117 how the properties of *collections* of documents change over time, our sliding window approach
118 allows us to examine the topic dynamics within a single document (or video). Specifically, our
119 approach yielded (via the topic proportions matrix) a single *topic vector* for each timepoint of the
120 episode (we set timepoints to match the acquisition times of the 1976 fMRI volumes collected as
121 participants viewed the episode).

122 The topics we found were heavily character-focused (e.g., the top-weighted word in each topic
123 was nearly always a character) and could be roughly divided into themes that were primarily
124 Sherlock Holmes-focused (Sherlock is the titular character), primarily John Watson-focused (John
125 is Sherlock’s close confidant and assistant), or focused on Sherlock and John interacting (Fig. S2).
126 Several of the topics were highly similar, which we hypothesized might allow us to distinguish
127 between subtle narrative differences (if the distinctions between those overlapping topics were



Figure 1: Methods overview. We used hand-annotated descriptions of each moment of video to fit a topic model. Three example video frames and their associated descriptions are displayed (top two rows). Participants later recalled the video (in the third row, we show example recalls of the same three scenes from participant 13). We used the topic model (fit to the annotations) to estimate topic vectors for each moment of video and each sentence the participants recalled. Example topic vectors are displayed in the bottom row (blue: video annotations; green: example participant’s recalls). Three topic dimensions are shown (the highest-weighted topics for each of the three example scenes, respectively). We also show the ten highest-weighted words for each topic. Figure S2 provides a full list of the top 10 words from each of the discovered topics.

128 meaningful; also see Fig. S3). The topic vectors for each timepoint were *sparse*, in that only a small
129 number (usually one or two) of topics tended to be “active” in any given timepoint (Fig. 2A).
130 Further, the dynamics of the topic activations appeared to exhibit *persistance* (i.e., given that a
131 topic was active in one timepoint, it was likely to be active in the following timepoint) along with
132 *occasional rapid changes* (i.e., occasionally topics would appear to spring into or out of existence).
133 These two properties of the topic dynamics may be seen in the block diagonal structure of the
134 timepoint-by-timepoint correlation matrix (Fig. 2B) and reflect the gradual drift and sudden shifts
135 fundamental to the contextual dynamics of real-world experiences. Given this observation, we
136 adapted an approach devised by Baldassano et al. (2017), and used a Hidden Markov Model (HMM)
137 to identify the *event boundaries* where the topic activations changed rapidly (i.e., at the boundaries
138 of the blocks in the correlation matrix; event boundaries identified by the HMM are outlined in
139 yellow). Part of our model fitting procedure required selecting an appropriate number of “events”
140 to segment the timeseries into. We used an optimization procedure to identify the number of
141 events that maximized within-event stability while also minimizing across-event correlations (see
142 *Methods* for additional details). To create a stable “summary” of the video, we computed the
143 average topic vector within each event (Fig. 2C).

144 Given that the time-varying content of the video could be segmented cleanly into discrete
145 events, we wondered whether participants’ recalls of the video also displayed a similar structure.
146 We applied the same topic model (already trained on the video annotations) to each participant’s
147 recalls. Analogous to how we analyzed the time-varying content of the video, to obtain similar
148 estimates for participants’ recalls, we treated each (overlapping) 10-sentence “window” of their
149 transcript as a “document” and then computed the most probable mix of topics reflected in each
150 timepoint’s sentences. This yielded, for each participant, a number-of-sentences by number-of-
151 topics topic proportions matrix that characterized how the topics identified in the original video
152 were reflected in the participant’s recalls. Note that an important feature of our approach is
153 that it allows us to compare participant’s recalls to events from the original video, despite that
154 different participants may have used different language to describe the same event, and that those
155 descriptions may not match the original annotations. This is a substantial benefit of projecting

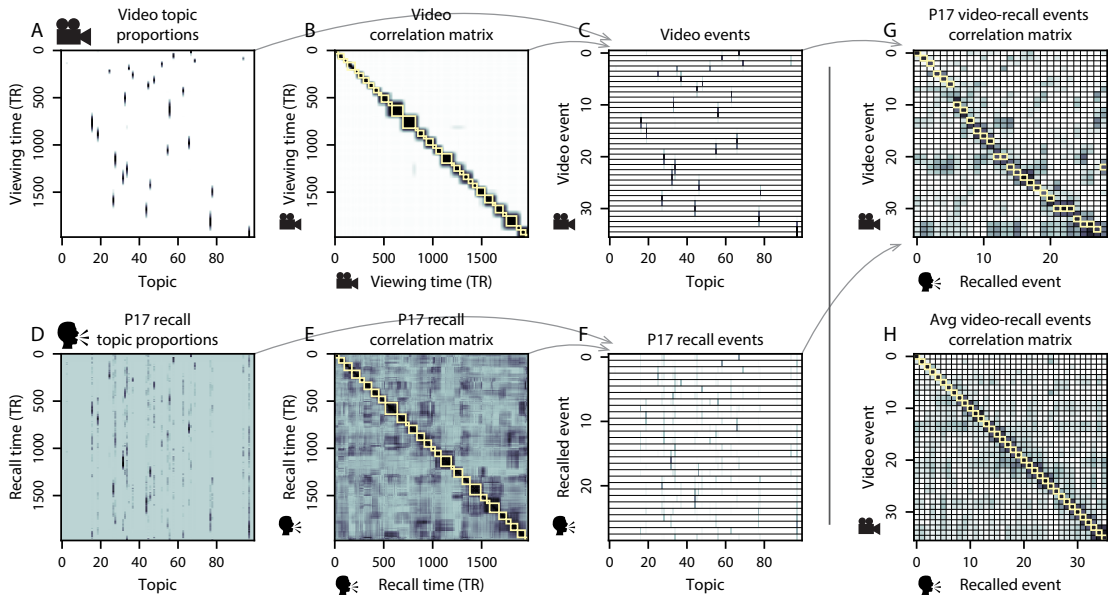


Figure 2: Modelling naturalistic stimuli and recalls. All panels: darker colors indicate greater values; range: [0, 1]. **A.** Topic vectors ($K = 100$) for each of the 1976 video timepoints. **B.** Timepoint-by-timepoint correlation matrix of the topic vectors displayed in Panel A. Event boundaries detected by the HMM are denoted in yellow (36 events detected). **C.** Average topic vectors for each of the 36 video events. **D.** Topic vectors for each of 252 sentences spoken by an example participant while recalling the video, resampled to match the timeseries of the video. **E.** Timepoint-by-timepoint correlation matrix of the topic vectors displayed in Panel D. Event boundaries detected by the HMM are denoted in yellow (29 events detected). **F.** Average topic vectors for each of the 29 recalled events from the example participant. **G.** Correlations between the topic vectors for every pair of video events (Panel C) and recalled events (from the example participant; Panel F). For similar plots for all participants see Figure S5. **H.** Average correlations between each pair of video events and recalled events (across all 17 participants). To create the figure, each recalled event was assigned to the video event with the most correlated topic vector (yellow boxes in panels G and H). The heat maps in each panel were created using Seaborn (Waskom et al., 2016).

156 the video and recalls into a shared “topic” space. An example topic proportions matrix from one
157 participant’s recalls is shown in Figure 2D.

158 Although the example participant’s recall topic proportions matrix has some visual similarity to
159 the video topic proportions matrix, the time-varying topic proportions for the example participant’s
160 recalls are not as sparse as for the video (e.g., compare Figs. 2A and D). Similarly, although there
161 do appear to be periods of stability in the recall topic dynamics (e.g., most topics are active or
162 inactive over contiguous blocks of time), the overall timecourses are not as cleanly delineated as
163 the video topics are. To examine these patterns in detail, we computed the timepoint-by-timepoint
164 correlation matrix for the example participant’s recall topic proportions (Fig. 2E). As in the video
165 correlation matrix (Fig. 2B), the example participant’s recall correlation matrix has a strong block
166 diagonal structure, indicating that their recalls are discretized into separated events. As for the
167 video correlation matrix, we can use an HMM, along with the aforementioned number-of-events
168 optimization procedure (also see *Methods*) to determine how many events are reflected in the
169 participant’s recalls and where specifically the event boundaries fall (outlined in yellow). We
170 carried out a similar analysis on all 17 participants’ recall topic proportions matrices (Fig. S4).

171 Two clear patterns emerged from this set of analyses. First, although every individual partic-
172 ipant’s recalls could be segmented into discrete events (i.e., every individual participant’s recall
173 correlation matrix exhibited clear block diagonal structure; Fig. S4), each participant appeared to
174 have a unique *recall resolution*, reflected in the sizes of those blocks. For example, some participants’
175 recall topic proportions segmented into just a few events (e.g., Participants P2, P6, and P14), while
176 others’ recalls segmented into many shorter duration events (e.g., Participants P12, P13, and P17).
177 This suggests that different participants may be recalling the video with different levels of detail-
178 e.g., some might touch on just the major plot points, whereas others might attempt to recall every
179 minor scene or action. The second clear pattern present in every individual participant’s recall
180 correlation matrix is that, unlike in the video correlation matrix, there are substantial off-diagonal
181 correlations. Whereas each event in the original video was (largely) separable from the others
182 (Fig. 2B), in transforming those separable events into memory, participants appear to be integrat-
183 ing across multiple events, blending elements of previously recalled and not-yet-recalled events

184 into each newly recalled event (Figs. 2D, S4; also see Manning et al., 2011; Howard et al., 2012).

185 The above results indicate that both the structure of the original video and participants' recalls
186 of the video exhibit event boundaries that can be identified automatically by characterizing the
187 dynamic content using a shared topic model and segmenting the content into events using HMMs.
188 Next, we asked whether some correspondence might be made between the specific content of the
189 events the participants experienced in the video, and the events they later recalled. One approach
190 to linking the experienced (video) and recalled events is to label each recalled event as matching
191 the video event with the most similar (i.e., most highly correlated) topic vector (Figs. 2G, S5). This
192 yields a sequence of "presented" events from the original video, and a (potentially differently
193 ordered) sequence of "recalled" events for each participant. Analogous to classic list-learning
194 studies, we can then examine participants' recall sequences by asking which events they tended
195 to recall first (probability of first recall; Fig. 3A; Welch and Burnett, 1924; Postman and Phillips,
196 1965; Atkinson and Shiffrin, 1968); how participants most often transition between recalls of the
197 events as a function of the temporal distance between them (lag-conditional response probability;
198 Fig. 3B; Kahana, 1996); and which events they were likely to remember overall (serial position
199 recall analyses; Fig. 3C; Murdock, 1962). Interestingly, for two of these analyses (probability of first
200 recall and lag-conditional response probability curves) we observe patterns comparable to classic
201 effects from the list-learning literature: namely, a higher probability of initiating recall with the
202 first event in the sequence (Fig. 3A) and a higher probability of transitioning to neighboring events
203 with an asymmetric forward bias (Fig. 3C). In contrast, we do not observe a pattern comparable to
204 the serial position effect (Fig. 3C), but rather we see higher memory for specific events distributed
205 somewhat evenly throughout the video.

206 We can also apply two list-learning-native analyses that describe how participants group items
207 in their recall sequences: temporal clustering and semantic clustering (Polyn et al., 2009, see
208 *Methods* for details). Temporal clustering refers to the extent to which participants group their
209 recall responses according to encoding position. Semantic clustering measures the extent to which
210 participants cluster their recall responses according to semantic similarity. Overall, we found that
participants heavily clustered video events in their recalls by both temporal proximity (mean:

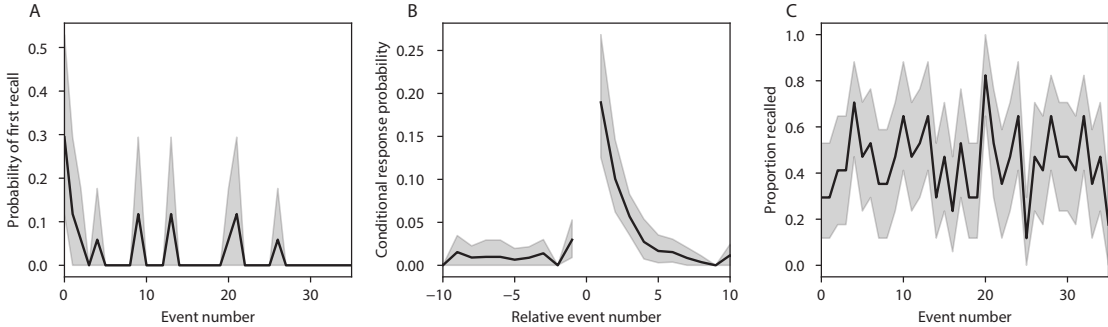


Figure 3: Naturalistic extensions of classic list-learning memory analyses. **A.** The probability of first recall as a function of the serial position of the event in the video. **B.** The probability of recalling each event, conditioned on having most recently recalled the event *lag* events away in the video. **C.** The proportion of participants who recalled each event, as a function of the serial position of the events in the video. All panels: error bars denote bootstrap-estimated standard error of the mean.

212 0.860, SEM: 0.016) and semantic content (mean: 0.888, SEM: 0.014).

213 Statistical models of memory studies often treat memory recalls as binary (e.g. the item was re-
 214 called or not) and independent events. However, our framework produces a content-based model
 215 of individual stimulus and recall events, allowing for direct quantitative comparison between all
 216 stimulus and recall events, as well as between the recall events themselves. Leveraging these
 217 content-based models of the stimulus/recall events, we developed two novel metrics for quanti-
 218 fying naturalistic memory representations: *precision* and *distinctiveness*. We define precision as the
 219 average correlation between the topic proportions of each recall event and the maximally corre-
 220 lated video event (Fig. 4). Participants whose recall events are more veridical descriptions of what
 221 happened in the video event will presumably have higher precision scores. We find that, across
 222 participants, a higher precision score is correlated to both hand-annotated memory performance
 223 (Pearson's $r(15) = 0.55, p = 0.021$) and the number of recall events estimated by our model (Pear-
 224 son's $r(15) = 0.66, p = 0.004$). A second novel metric we introduce here is distinctiveness, or how
 225 unique the recall description was to each video event. We define distinctiveness as 1 minus the av-
 226 erage of all non-matching recall events from the video-recall correlation matrix. We hypothesized
 227 that participants who recounted events in a more distinctive way would display better overall
 228 memory. Similarly to precision, we find that the more distinct participants recalls are (on average),

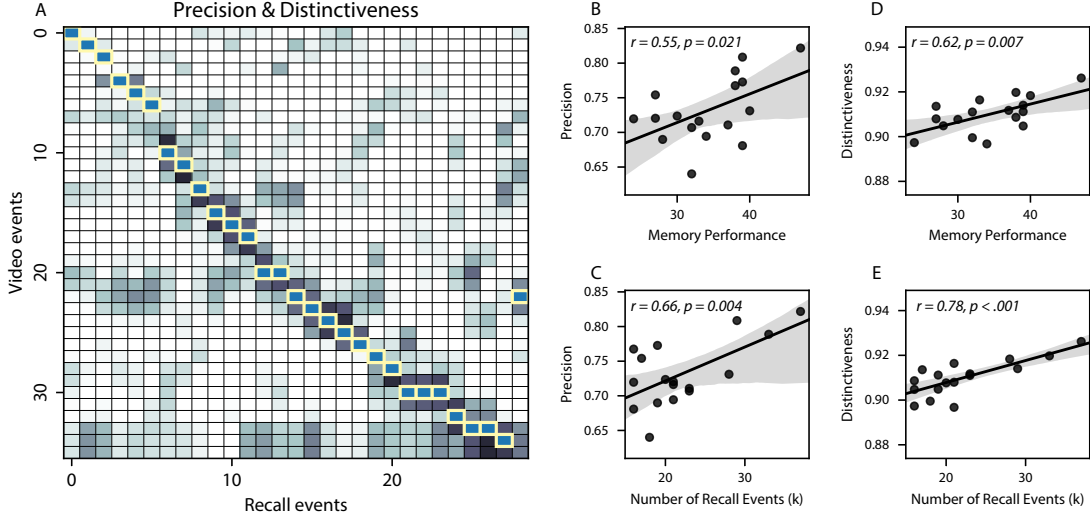


Figure 4: Novel content-based metrics of naturalistic memory: precision and distinctiveness. **A.** A video-recall correlation matrix for a representative participant (17). The yellow boxes highlight the maximum correlation in each column. Precision was computed as the average of the maximum correlation in each column. On the other hand, distinctiveness was defined as the average of everything except for the maximum correlation in each column. **B.** The (Pearson's) correlation between precision and hand-annotated memory performance. **C.** The correlation between precision and the number of events recovered by the model (k). **D.** The correlation between distinctiveness and hand-annotated memory performance. **E.** The correlation between distinctiveness and the number of events recovered by the model (k).

the more they remembered (hand-annotated memory: Pearson's $r(15) = 0.62, p = 0.007$; number of events: Pearson's $r(15) = 0.78, p < 0.001$). In summary, using two novel metrics afforded by our approach, we find that participants whose recalls are both more precise and distinct remember more content.

The prior analyses leverage the correspondence between the 100-dimensional topic proportion matrices for the video and participants' recalls to characterize recall. However, it is difficult to gain deep insights into that content solely by examining the topic proportion matrices (e.g., Figs. 2A, D) or the corresponding correlation matrices (Figs. 2B, E, S4). To visualize the time-varying high-dimensional content in a more intuitive way (Heusser et al., 2018b) we projected the topic proportions matrices onto a two-dimensional space using Uniform Manifold Approximation and Projection (UMAP; McInnes and Healy, 2018). In this lower-dimensional space, each point

240 represents a single video or recall event, and the distances between the points reflect the distances
241 between the events' associated topic vectors (Fig. 5). In other words, events that are near to each
242 other in this space are more semantically similar.

243 Visual inspection of the video and recall topic trajectories reveals a striking pattern. First,
244 the topic trajectory of the video (which reflects its dynamic content; Fig. 5A) is captured nearly
245 perfectly by the averaged topic trajectories of participants' recalls (Fig. 5B). To assess the consistency
246 of these recall trajectories across participants, we asked: given that a participant's recall trajectory
247 had entered a particular location in topic space, could the position of their *next* recalled event
248 be predicted reliably? For each location in topic space, we computed the set of line segments
249 connecting successively recalled events (across all participants) that intersected that location (see
250 *Methods* for additional details). We then computed (for each location) the distribution of angles
251 formed by the lines defined by those line segments and a fixed reference line (the *x*-axis). Rayleigh
252 tests revealed the set of locations in topic space at which these across-participant distributions
253 exhibited reliable peaks (blue arrows in Fig. 5B reflect significant peaks at $p < 0.05$, corrected). We
254 observed that the locations traversed by nearly the entire video trajectory exhibited such peaks.
255 In other words, participants exhibited similar trajectories that also matched the trajectory of the
256 original video (Fig. 5C). This is especially notable when considering the fact that the number of
257 events participants recalled (dots in Fig. 5C) varied considerably across people, and that every
258 participant used different words to describe what they had remembered happening in the video.
259 Differences in the numbers of remembered events appear in participants' trajectories as differences
260 in the sampling resolution along the trajectory. We note that this framework also provides a
261 means of detangling classic "proportion recalled" measures (i.e., the proportion of video events
262 referenced in participants' recalls) from participants' abilities to recapitulate the full shape of the
263 original video (i.e., the similarity in the shape of the original video trajectory and that defined by
264 each participant's recounting of the video).

265 Because our analysis framework projects the dynamic video content and participants' recalls
266 onto a shared topic space, and because the dimensions of that space are known (i.e., each topic
267 dimension is a set of weights over words in the vocabulary; Fig. S2), we can examine the topic

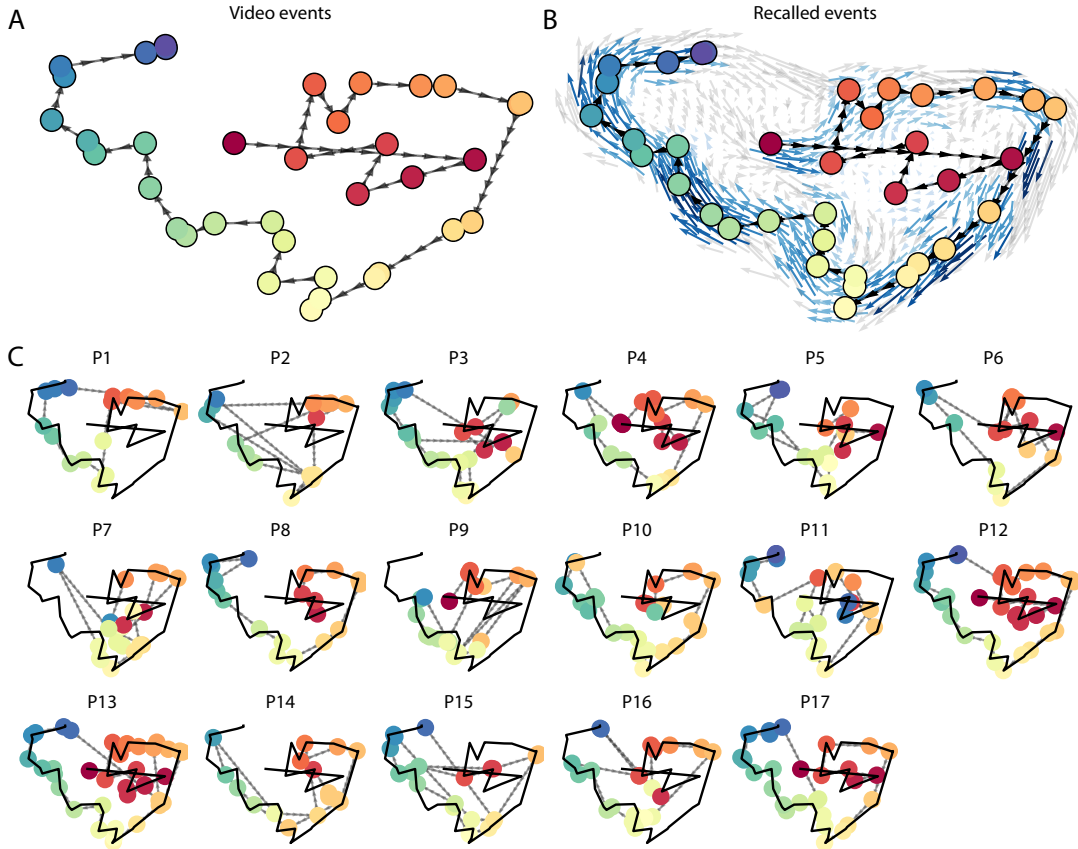


Figure 5: Trajectories through topic space capture the dynamic content of the video and recalls. All panels: the topic proportion matrices have been projected onto a shared two-dimensional space using UMAP. **A.** The two-dimensional topic trajectory taken by the episode of *Sherlock*. Each dot indicates an event identified using the HMM (see *Methods*); the dot colors denote the order of the events (early events are in red; later events are in blue), and the connecting lines indicate the transitions between successive events. **B.** The average two-dimensional trajectory captured by participants' recall sequences, with the same format and coloring as the trajectory in Panel A. To compute the event positions, we matched each recalled event with an event from the original video (see *Results*), and then we averaged the positions of all events with the same label. The arrows reflect the average transition direction through topic space taken by any participants whose trajectories crossed that part of topic space; blue denotes reliable agreement across participants via a Rayleigh test ($p < 0.05$, corrected). **C.** The recall topic trajectories (gray) taken by each individual participant (P1–P17). The video's trajectory is shown in black for reference. (Same format and coloring as Panel A.)

268 trajectories to understand which specific content was remembered well (or poorly). For each video
269 event, we can ask: what was the average correlation (across participants) between the video event's
270 topic vector and the closest matching recall event topic vectors from each participant? This yields a
271 single correlation coefficient for each video event, describing how closely participants' recalls of the
272 event tended to reliably capture its content (Fig. 6A). (We also examined how different comparisons
273 between each video event's topic vector and the corresponding recall event topic vectors related
274 to hand-annotated characterizations of memory performance; see *Supporting Information*). Given
275 this summary of which events were recalled reliably (or not), we next asked whether the better-
276 remembered or worse-remembered events tended to reflect particular topics. We computed a
277 weighted average of the topic vectors for each video event, where the weights reflected how
278 reliably each event was recalled. To visualize the result, we created a "wordle" image (Mueller
279 et al., 2018) where words weighted more heavily by better-remembered topics appear in a larger
280 font (Fig. 6B, green box). Across the full video, content that reflected topics necessary to convey
281 the central focus of the video (e.g., the names of the two main characters, "Sherlock" and "John",
282 and the address of a major recurring location, "221b Baker Street") were best remembered. An
283 analogous analysis revealed which themes were poorly remembered. Here in computing the
284 weighted average over events' topic vectors, we weighted each event in *inverse* proportion to how
285 well it was remembered (Fig. 6B, red box). The least well-remembered video content reflected
286 information not necessary to conveying the video's "gist," such as the names of relatively minor
287 characters (e.g., "Mike," "Jeffrey," "Molly," and "Jimmy") and locations (e.g., "St. Bartholomew's
288 Hospital").

289 A similar result emerged from assessing the topic vectors for individual video and recall events
290 (Fig. 6C). Here, for each of the three best- and worst-remembered video events, we have constructed
291 two wordles: one from the original video event's topic vector (left) and a second from the average
292 recall topic vector for that event (right). The three best-remembered events (circled in green)
293 correspond to scenes important to the central plot-line (Sherlock and John meeting, Sherlock and
294 John chasing the killer, and the killer calling spying on John in a phone booth). Meanwhile, the three
295 worst-remembered events (circled in red) reflect various side-stories (John talking to his therapist

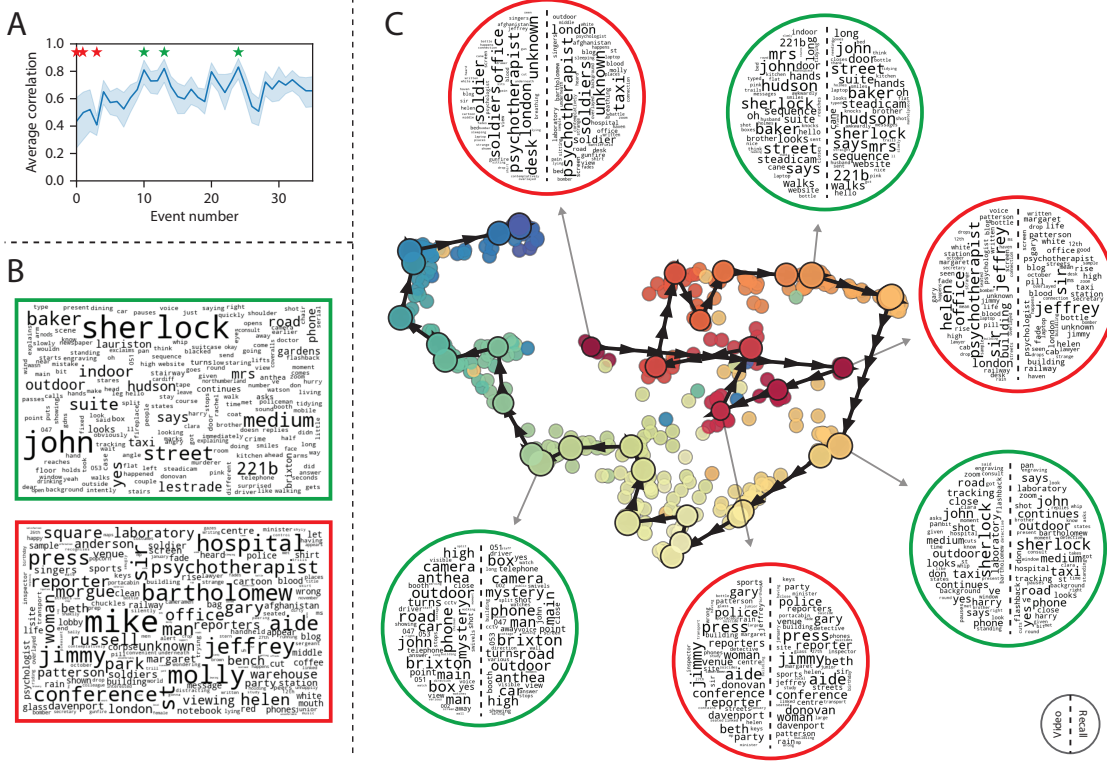


Figure 6: Transforming experience into memory. **A.** Average correlations (across participants) between the topic vectors from each video event and the closest-matching recall events. Error bars denote bootstrap-derived across-participant 95% confidence intervals. The stars denote the three best-remembered events (green) and worst-remembered events (red). **B.** Wordles comprising the top 200 highest-weighted words reflected in the weighted-average topic vector across video events. Green: video events were weighted by how well the topic vectors derived from recalls of those events matched the video events' topic vectors (Panel A). Red: video events were weighted by the inverse of how well their topic vectors matched the recalled topic vectors. **C.** The set of all video and recall events is projected onto the two-dimensional space derived in Figure 5. The dots outlined in black denote video events (dot size reflects the average correlation between the video event's topic vector and the topic vectors from the closest matching recalled events from each participant; bigger dots denote stronger correlations). The dots without black outlines denote recalled events. All dots are colored using the same scheme as Figure 5A. Wordles for several example events are displayed (green: three best-remembered events; red: three worst-remembered events). Within each circular wordle, the left side displays words associated with the topic vector for the video event, and the right side displays words associated with the (average) recall event topic vector, across all recall events matched to the given video event.

296 about the war, a soon-to-be-victim's affair with his assistant, and another soon-to-be-victim leaving
297 a party with his friend) that are not essentially to summarizing the video's narrative.

298 The results thus far inform us about which aspects of the dynamic content in the episode
299 participants watched were preserved or altered in participants' memories of the episode. We next
300 carried out a series of analyses aimed at understanding which brain structures might implement
301 these processes. In one analysis we sought to identify which brain structures were sensitive
302 to the video's dynamic content, as characterized by its topic trajectory. Specifically, we used a
303 searchlight procedure to identify the extent to which each cluster of voxels exhibited a timecourse
304 of activity (as the participants watched the video) whose temporal correlation matrix matched
305 the temporal correlation matrix of the original video's topic proportions (Fig. 2B). As shown
306 in Figure 7A, the analysis revealed a network of regions including bilateral frontal cortex and
307 cingulate cortex, suggesting that these regions may play a role in processing information relevant
308 to the narrative structure of the video. In a second analysis, we sought to identify which brain
309 structures' responses (while viewing the video) reflected how each participant would later *recall*
310 the video. We used an analogous searchlight procedure to identify clusters of voxels whose
311 temporal correlation matrices reflected the temporal correlation matrix of the topic proportions for
312 each individual's recalls (Figs. 2D, S4). As shown in Figure 7B, the analysis revealed a network of
313 regions including the ventromedial prefrontal cortex (vmPFC), anterior cingulate cortex (ACC), and
314 right medial temporal lobe (rMTL), suggesting that these regions may play a role in transforming
315 each individual's experience into memory. In identifying regions whose responses to ongoing
316 experiences reflect how those experiences will be remembered later, this latter analysis extends
317 classic *subsequent memory analyses* (e.g., Paller and Wagner, 2002) to domain of naturalistic stimuli.

318 Discussion

319 Our work casts remembering as reproducing (behaviorally and neurally) the topic trajectory, or
320 shape, of an experience. This view draws inspiration from prior work aimed at elucidating
321 the neural and behavioral underpinnings of how we process dynamic naturalistic experiences

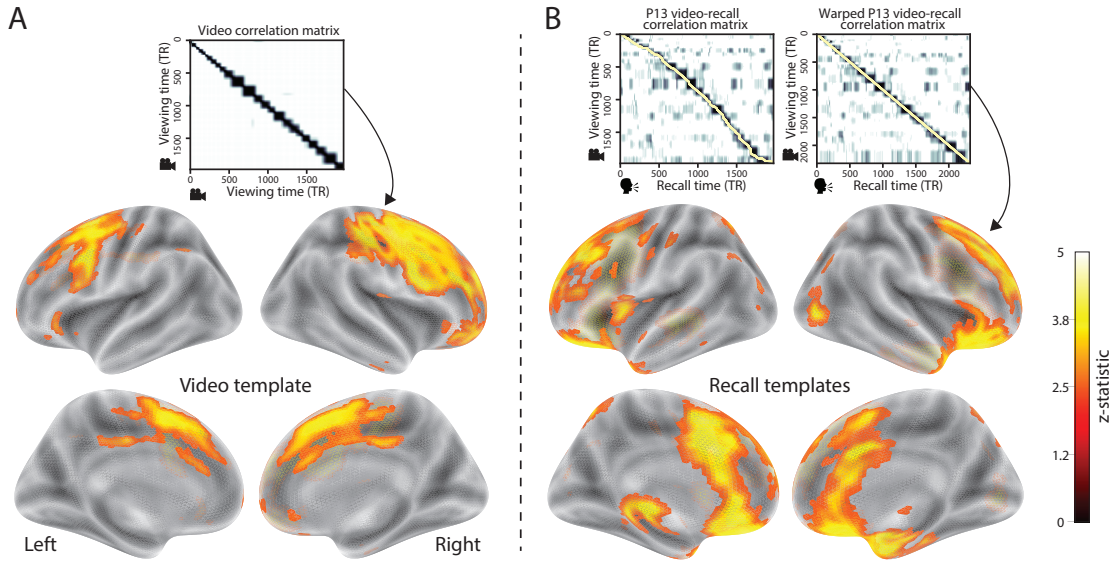


Figure 7: Brain structures that underlie the transformation of experience into memory. **A.** We searched for regions whose responses (as participants watched the video) matched the temporal correlation matrix of the video topic proportions. These regions are sensitive to the narrative structure of the video. **B.** We searched for regions whose responses (as participants watched the video) matched the temporal correlation matrix of the topic proportions derived from each individual's later recall of video. These regions are sensitive to how the narrative structure of the video is transformed into a memory of the video. Both panels: the maps are thresholded at $p < 0.05$, corrected.

and remember them later. One approach to identifying neural responses to naturalistic stimuli (including experiences) entails building a model of the stimulus and searching for brain regions whose responses are consistent with the model. In prior work, a series of studies from Uri Hasson's group (Lerner et al., 2011; Simony et al., 2016; Chen et al., 2017; Baldassano et al., 2017; Zadbood et al., 2017) have extended this approach with a clever twist: rather than building an explicit stimulus model, these studies instead search for brain responses (while experiencing the stimulus) that are reliably similar across individuals. So called *inter-subject correlation* (ISC) and *inter-subject functional connectivity* (ISFC) analyses effectively treat other people's brain responses to the stimulus as a "model" of how its features change over time. By contrast, in our present work we used topic models and HMMs to construct an explicit stimulus model (i.e., the topic trajectory of the video). When we searched for brain structures whose responses are consistent with the video's topic trajectory, we identified a network of structures that overlapped strongly with the "long temporal receptive window" network reported by the Hasson group (e.g., compare our Fig. 7A with the map of long temporal receptive window voxels in Lerner et al., 2011). This provides support for the notion that part of the long temporal receptive window network may be maintaining an explicit model of the stimulus dynamics. When we performed a similar analysis after swapping out the video's topic trajectory with the recall topic trajectories of each individual participant, this allowed us to identify brain regions whose responses (as the participants viewed the video) reflected how the video trajectory would be transformed in memory (as reflected by the recall topic trajectories). The analysis revealed that the rMTL and vmPFC may play a role in this person-specific transformation from experience into memory. The role of the MTL in episodic memory encoding has been well-reported (e.g., Paller and Wagner, 2002; Davachi et al., 2003; Ranganath et al., 2004; Davachi, 2006; Wiltgen and Silva, 2007; Diana et al., 2007; van Kesteren et al., 2013). Prior work has also implicated the medial prefrontal cortex in representing "schema" knowledge (i.e., general knowledge about the format of an ongoing experience given prior similar experiences; van Kesteren et al., 2012, 2013; Schlichting and Preston, 2015; Gilboa and Marlatte, 2017; Spalding et al., 2018). Integrating across our study and this prior work, one interpretation is that the person-specific transformations mediated (or represented) by the rMTL and vmPFC may

350 reflect schema knowledge being leveraged, formed, or updated, incorporating ongoing experience
351 into previously acquired knowledge.

352 In extending classical free recall analyses to our naturalistic memory framework, we recovered
353 two patterns of recall dynamics central to list-learning studies: a high probability of initiating
354 recall with the first video event (Fig. 3A) and a strong bias toward transitioning from recalling a
355 given event to recalling the event immediately following it (Fig. 3B). However, equally noteworthy
356 are the typical free recall results not recovered in these analyses, as each highlights a fundamental
357 difference between list-learning studies and naturalistic memory paradigms like the one employed
358 in the present study. The most noticeable departure from hallmark free recall dynamics in these
359 findings is the apparent lack of a serial position effect in Figure 3C, which instead shows greater
360 and lesser recall probabilities for events distributed across the video stimulus. Stimuli in free recall
361 experiments most often comprise lists of simple, common words, presented to participants in a
362 random order. (In fact, numerous word pools have been developed based on these criteria; e.g.,
363 Friendly et al., 1982). These stimulus qualities enable two assumptions that are central to word
364 list analyses, but frequently do not hold for real-world experiences. First, researchers conducting
365 free recall studies may assume that the content at each presentation index is essentially equal, and
366 does not bear qualities that would cause participants to remember it more or less successfully than
367 others. Such is rarely the case with real-world experiences or experiments meant to approximate
368 them, and the effects of both intrinsic and observer-dependent factors on stimulus memorability
369 are well established (for review see Chun and Turk-Browne, 2007; Bylinskii et al., 2015; Tyng
370 et al., 2017). Second, the random ordering of list items ensures that (across participants, on
371 average) there is no relationship between the thematic similarity of individual stimuli and their
372 presentation positions—in other words, two semantically related words are no more likely to be
373 presented next to each other than at opposite ends of the list. In most cases, the exact opposite
374 is true of real-world episodes. Our internal thoughts, our actions, and the physical state of the
375 world around us all tend to follow a direct, causal progression. As a result, each moment of our
376 experience tends to be inherently more similar to surrounding moments than to those in the distant
377 past or future. Memory literature has termed this strong temporal autocorrelation “context,” and

378 in various media that depict real-world events (e.g., movies and written stories), we recognize
379 it as a *narrative structure*. While a random word list (by definition) has no such structure, the
380 logical progression between ideas and actions in a naturalistic stimulus prompts the rememberer
381 to recount presented events in order, starting with the beginning. This tendency is reflected in our
382 findings' second departure from typical free recall dynamics: a lack of increased probability of first
383 recall for end-of-sequence events (Fig. 3A).

384 Thus, analyses such as those in Figure 3 that address only the temporal dynamics of free re-
385 call paint an incomplete picture of memory for naturalistic episodes. While useful for studying
386 presentation order-dependent recall dynamics, they neglect to consider the stimuli's content (or,
387 for example, that content's potential interrelatedness). However, sensitivity to stimulus and recall
388 content introduces a new challenge: distinguishing between levels of recall quality for a stimulus
389 (i.e., an event) that is considered to have been "remembered." When modeling memory experi-
390 ments, often times events (or items) and their later memories are treated as binary and independent
391 events (e.g., a given list item was simply either remembered or not remembered). Various models
392 of memory (e.g., Yonelinas, 2002) attempt to improve upon this by including confidence ratings,
393 rendering this binary judgement instead categorical. Our novel framework allows one to assess
394 memory performance in a more continuous way (*precision*), as well as analyze the correlational
395 structure of each encoding event to each memory event (*distinctiveness*). Further and importantly,
396 these two novel metrics we introduce here arise from comparisons of the actual content of the
397 experience/memories, which is not typically modeled. Leveraging this, we find that the successful
398 memory performance is related to 1) the precision with which the participant recounts each event
399 and 2) the distinctiveness of each recall event (relative to the other recalled events). The first finding
400 suggests that the information retained for *any individual event* may predict the overall amount of
401 information retained by the participant. The second finding suggests that the ability to distin-
402 guish between temporally or semantically similar content is also related to the quantity of content
403 recovered. Intriguingly, prior studies show that pattern separation, or the ability to discriminate
404 between similar experiences, is impaired in many cognitive disorders as well as natural aging
405 (Stark et al., 2010; Yassa et al., 2011; Yassa and Stark, 2011). Future work might explore whether

406 and how these metrics compare between cognitively impoverished groups and healthy controls.

407 While a large number of language models exist (e.g., WAS, LSA, word2vec, universal sentence
408 encoder; Steyvers et al., 2004; Landauer et al., 1998; Mikolov et al., 2013; Cer et al., 2018), here
409 we use latent dirichlet allocation (LDA)-based topic models for a few reasons. First, topic models
410 capture the *essence* of a text passage devoid of the specific set and order of words used. This
411 was an important feature of our model since different people may accurately recall a scene using
412 very different language. Second, words can mean different things in different contexts (e.g. "bat"
413 as the act of hitting a baseball, the object used for that action, or as a flying mammal). Topic
414 models are robust to this, allowing words to exist as part of multiple topics. Last, topic models
415 provide a straightforward means to recover the weights for the particular words comprising a topic,
416 enabling easy interpretation of an event's contents (e.g. Fig. 6). Other models such as Google's
417 universal sentence encoder offer a context-sensitive encoding of text passages, but the encoding
418 space is complex and non-linear, and thus recovering the original words used to fit the model is
419 not straightforward. However, it's worth pointing out that our framework is divorced from the
420 particular choice of language model. Moreover, many of the aspects of our framework could be
421 swapped out for other choices. For example, the language model, the timeseries segmentation
422 model and the video-recall matching function could all be customized for the particular problem.
423 Indeed for some problems, recovery of the particular recall words may not be necessary, and thus
424 other text-modeling approaches (such as universal sentence encoder) may be preferable. Future
425 work will explore the influence of particular model choices on the framework's accuracy.

426 Our work has broad implications for how we characterize and assess memory in real-world
427 settings, such as the classroom or physician's office. For example, the most commonly used
428 classroom evaluation tools involve simply computing the proportion of correctly answered exam
429 questions. Our work indicates that this approach is only loosely related to what educators might
430 really want to measure: how well did the students understand the key ideas presented in the
431 course? Under this typical framework of assessment, the same exam score of 50% could be
432 ascribed to two very different students: one who attended the full course but struggled to learn
433 more than a broad overview of the material, and one who attended only half of the course but

434 understood the material perfectly. Instead, one could apply our computational framework to build
435 explicit content models of the course material and exam questions. This approach would provide
436 a more nuanced and specific view into which aspects of the material students had learned well
437 (or poorly). In clinical settings, memory measures that incorporate such explicit content models
438 might also provide more direct evaluations of patients' memories.

439 **Methods**

440 **Experimental design and data collection**

441 Data were collected by Chen et al. (2017). In brief, participants ($n = 17$) viewed the first 48 minutes
442 of "A Study in Pink", the first episode of the BBC television series *Sherlock*, while fMRI volumes
443 were collected (TR = 1500 ms). The stimulus was divided into a 23 min (946 TR) and a 25 min
444 (1030 TR) segment to mitigate technical issues related to the scanner. After finishing the clip,
445 participants were instructed to (quoting from Chen et al., 2017) "describe what they recalled of the
446 [episode] in as much detail as they could, to try to recount events in the original order they were
447 viewed in, and to speak for at least 10 minutes if possible but that longer was better. They were told
448 that completeness and detail were more important than temporal order, and that if at any point
449 they realized they had missed something, to return to it. Participants were then allowed to speak
450 for as long as they wished, and verbally indicated when they were finished (e.g., 'I'm done')."
451 For additional details about the experimental procedure and scanning parameters, see Chen et al.
452 (2017). The experimental protocol was approved by Princeton University's Institutional Review
453 Board.

454 After preprocessing the fMRI data and warping the images into a standard (3 mm³ MNI) space,
455 the voxel activations were z-scored (within voxel) and spatially smoothed using a 6 mm (full width
456 at half maximum) Gaussian kernel. The fMRI data were also cropped so that all video-viewing
457 data were aligned across participants. This included a constant 3 TR (4.5 s) shift to account for the
458 lag in the hemodynamic response. (All of these preprocessing steps followed Chen et al., 2017,

459 where additional details may be found.)

460 **Data and code availability**

461 The fMRI data we analyzed are available online [here](#). The behavioral data and all of our analysis
462 code may be downloaded [here](#).

463 **Statistics**

464 All statistical tests we performed were two-sided.

465 **Modeling the dynamic content of the video and recall transcripts**

466 **Topic modeling**

467 The input to the topic model we trained to characterize the dynamic content of the video comprised
468 hand-generated annotations of each of 1000 scenes spanning the video clip (generated by Chen
469 et al., 2017). The features annotated included: narrative details (a sentence or two describing
470 what happened in that scene); whether the scene took place indoors or outdoors; names of any
471 characters that appeared in the scene; name(s) of characters in camera focus; name(s) of characters
472 who were speaking in the scene; the location (in the story) that the scene took place; camera angle
473 (close up, medium, long, top, tracking, over the shoulder, etc.); whether music was playing in
474 the scene or not; and a transcription of any on-screen text. We concatenated the text for all of
475 these features within each segment, creating a “bag of words” describing each scene. We then
476 re-organized the text descriptions into overlapping sliding windows spanning 50 scenes each.
477 In other words, the first text sample comprised the combined text from the first 50 scenes (i.e.,
478 1–50), the second comprised the text from scenes 2–51, and so on. We trained our model using
479 these overlapping text samples with `scikit-learn` (version 0.19.1; Pedregosa et al., 2011), called
480 from our high-dimensional visualization and text analysis software, `HyperTools` (Heusser et al.,
481 2018b). Specifically, we used the `CountVectorizer` class to transform the text from each scene
482 into a vector of word counts (using the union of all words across all scenes as the “vocabulary,”

483 excluding English stop words); this yielded a number-of-scenes by number-of-words *word count*
484 matrix. We then used the `LatentDirichletAllocation` class (`topics=100`, `method='batch'`) to fit
485 a topic model (Blei et al., 2003) to the word count matrix, yielding a number-of-scenes (1000) by
486 number-of-topics (100) *topic proportions* matrix. The topic proportions matrix describes which mix
487 of topics (latent themes) is present in each scene. Next, we transformed the topic proportions
488 matrix to match the 1976 fMRI volume acquisition times. For each fMRI volume, we took the topic
489 proportions from whatever scene was displayed for most of that volume's 1500 ms acquisition time.
490 This yielded a new number-of-TRs (1976) by number-of-topics (100) topic proportions matrix.

491 We created similar topic proportions matrices using hand-annotated transcripts of each par-
492 ticipant's recall of the video (annotated by Chen et al., 2017). We tokenized the transcript into
493 a list of sentences, and then re-organized the list into overlapping sliding windows spanning 10
494 sentences each; in turn we transformed each window's sentences into a word count vector (using
495 the same vocabulary as for the video model). We then used the topic model already trained on
496 the video scenes to compute the most probable topic proportions for each sliding window. This
497 yielded a number-of-sentences (range: 68–294) by number-of-topics (100) topic proportions matrix,
498 for each participant. These reflected the dynamic content of each participant's recalls. Finally, we
499 resampled each recall model to match the timecourse of the video model. Note: for details on how
500 we selected the video and recall window lengths and number of topics, see *Supporting Information*
501 and Figure S1.

502 **Parsing topic trajectories into events using Hidden Markov Models**

503 We parsed the topic trajectories of the video and participants' recalls into events using Hidden
504 Markov Models (Rabiner, 1989). Given the topic proportions matrix (describing the mix of topics
505 at each timepoint) and a number of states, K , an HMM recovers the set of state transitions that
506 segments the timeseries into K discrete states. Following Baldassano et al. (2017), we imposed an
507 additional set of constraints on the discovered state transitions that ensured that each state was
508 encountered exactly once (i.e., never repeated). We used the BrainIAK toolbox (Capota et al., 2017)
509 to implement this segmentation.

510 We used an optimization procedure to select the appropriate K for each topic proportions
511 matrix. Specifically, we computed (for each matrix)

$$\operatorname{argmax}_K \left[POM\left(\frac{a}{b-J}\right) - \frac{K}{\alpha} \right],$$

512 where a was the average correlation between the topic vectors of timepoints within the same state;
513 b was the average correlation between the topic vectors of timepoints within *different* states; J was
514 a constant used to ensure a positive denominator, set equal to $\min_K \left[\frac{a}{b} \right]$; and α was a regularization
515 parameter that we set to 5 times the window length (i.e., 250 scenes for the video topic trajectory
516 and 50 sentences for the recall topic trajectories). Before subtracting the regularization term, we
517 scaled the ratio of correlations to be a proportion of the maximum ratio across all K 's. Figure 2B
518 displays the event boundaries returned for the video, and Figure S4 displays the event boundaries
519 returned for each participant's recalls (See Fig. S6 for the values of a and b for each K , Fig. S7 for
520 the optimization functions for the video and recalls). After obtaining these event boundaries, we
521 created stable estimates of each topic proportions matrix by averaging the topic vectors within
522 each event. This yielded a number-of-events by number-of-topics matrix for the video and recalls
523 from each participant.

524 We also evaluated a parameter-free procedure for choosing K , which finds the K value that
525 maximizes the Wasserstein distance (a.k.a. “Earth mover’s” distance) between the within and
526 across event distributions of correlation values. This alternative procedure largely replicated the
527 pattern of results found with the parameterized method described above, but recovered sub-
528 stantially fewer events on average (Fig.S8). While both approaches seem to underestimate the
529 number of video/recall events relative to the “true” number (as determined by human raters), the
530 parameterized approach was closer to the true number.

531 **Naturalistic extensions of classic list-learning analyses**

532 In traditional list-learning experiments, participants view a list of items (e.g., words) and then recall
533 the items later. Our video-recall event matching approach affords us the ability to analyze memory

534 in a similar way. The video and recall events can be treated analogously to studied and recalled
535 “items” in a list-learning study. We can then extend classic analyses of memory performance and
536 dynamics (originally designed for list-learning experiments) to the more naturalistic video recall
537 task used in this study.

538 Perhaps the simplest and most widely used measure of memory performance is *accuracy*—i.e.,
539 the proportion of studied (experienced) items (in this case, the 34 video events) that the participant
540 later remembered. Chen et al. (2017) developed a human rating system whereby the quality of
541 each participant’s memory was evaluated by an independent rater. We found a strong across-
542 participants correlation between these independant ratings and the overall number of events that
543 our HMM approach identified in participants’ recalls (Pearson’s $r(15) = 0.64, p = 0.006$).

544 As described below, we next considered a number of memory performance measures that are
545 typically associated with list-learning studies. We also provide a software package, Quail, for
546 carrying out these analyses (Heusser et al., 2017).

547 **Probability of first recall (PFR).** PFR curves (Welch and Burnett, 1924; Postman and Phillips,
548 1965; Atkinson and Shiffrin, 1968) reflect the probability that an item will be recalled first as a
549 function of its serial position during encoding. To carry out this analysis, we initialized a number-
550 of-participants (17) by number-of-video-events (34) matrix of zeros. Then for each participant, we
551 found the index of the video event that was recalled first (i.e., the video event whose topic vector
552 was most strongly correlated with that of the first recall event) and filled in that index in the matrix
553 with a 1. Finally, we averaged over the rows of the matrix, resulting in a 1 by 34 array representing
554 the proportion of participants that recalled an event first, as a function of the order of the event’s
555 appearance in the video (Fig. 3A).

556 **Lag conditional probability curve (lag-CRP).** The lag-CRP curve (Kahana, 1996) reflects the
557 probability of recalling a given event after the just-recalled event, as a function of their relative
558 positions (or *lag*). In other words, a lag of 1 indicates that a recalled event came immediately after
559 the previously recalled event in the video, and a lag of -3 indicates that a recalled event came 3

560 events before the previously recalled event. For each recall transition (following the first recall),
561 we computed the lag between the current recall event and the next recall event, normalizing by
562 the total number of possible transitions. This yielded a number-of-participants (17) by number-
563 of-lags (-33 to +33; 67 lags total) matrix. We averaged over the rows of this matrix to obtain a
564 group-averaged lag-CRP curve (Fig. 3B).

565 **Serial position curve (SPC).** SPCs (Murdock, 1962) reflect the proportion of participants that
566 remember each item as a function of the items' serial position during encoding. We initialized
567 a number-of-participants (17) by number-of-video-events (34) matrix of zeros. Then, for each
568 recalled event, for each participant, we found the index of the video event that the recalled event
569 most closely matched (via the correlation between the events' topic vectors) and entered a 1 into
570 that position in the matrix (i.e., for the given participant and event). This resulted in a matrix
571 whose entries indicated whether or not each event was recalled by each participant (depending
572 on whether the corresponding entires were set to one or zero). Finally, we averaged over the rows
573 of the matrix to yield a 1 by 34 array representing the proportion of participants that recalled each
574 event as a function of the order of the event's appearance in the video (Fig. 3C).

575 **Temporal clustering scores.** Temporal clustering describes participants' tendency to organize
576 their recall sequences by the learned items' encoding positions. For instance, if a participant
577 recalled the video events in the exact order they occurred (or in exact reverse order), this would
578 yield a score of 1. If a participant recalled the events in random order, this would yield an expected
579 score of 0.5. For each recall event transition (and separately for each participant), we sorted
580 all not-yet-recalled events according to their absolute lag (i.e., distance away in the video). We
581 then computed the percentile rank of the next event the participant recalled. We averaged these
582 percentile ranks across all of the participant's recalls to obtain a single temporal clustering score
583 for the participant.

584 **Semantic clustering scores.** Semantic clustering describes participants' tendency to recall seman-
585 tically similar presented items together in their recall sequences. Here, we used the topic vectors

586 for each event as a proxy for its semantic content. Thus, the similarity between the semantic
587 content for two events can be computed by correlating their respective topic vectors. For each
588 recall event transition, we sorted all not-yet-recalled events according to how correlated the topic
589 vector of the closest-matching video event was to the topic vector of the closest-matching video event
590 to the just-recalled event. We then computed the percentile rank of the observed next recall. We
591 averaged these percentile ranks across all of the participant's recalls to obtain a single semantic
592 clustering score for the participant.

593 **Novel naturalistic memory metrics**

594 **Precision.** We tested whether participants who recalled more events were also more *precise* in
595 their recollections. For each participant, we computed the average correlation between the topic
596 vectors for each recall event and those of its closest-matching video event. This gave a single value
597 per participant representing the average precision across all recalled events. We then Fisher's *z*-
598 transformed these values and correlated them with both hand-annotated and model-derived (i.e.,
599 k or the number of events recovered by the HMM) memory performance.

600 **Distinctiveness.** We also considered the *distinctiveness* of each recalled event. That is, how
601 uniquely a recalled event's topic vector matched a given video event topic vector, versus the
602 topic vectors for the other video events. We hypothesized that participants with high memory
603 performance might describe each event in a more distinctive way (relative to those with lower
604 memory performance who might describe events in a more general way). To test this hypothesis
605 we define a distinctiveness score for each recall event as

$$d(\text{event}) = 1 - \bar{c}(\text{event}),$$

606 where $\bar{c}(\text{event})$ is the average correlation between the given recalled event's topic vector and the
607 topic vectors from all video events *except* the best-matching video event. We then averaged these
608 distinctiveness scores across all of the events recalled by the given participant. As above, we used

609 Fisher's z -transformation before correlating these values with hand-annotated and model derived
610 memory performance scores across-subjects.

611 **Visualizing the video and recall topic trajectories**

612 We used the UMAP algorithm (McInnes and Healy, 2018) to project the 100-dimensional topic space
613 onto a two-dimensional space for visualization (Figs. 5, 6). To ensure that all of the trajectories were
614 projected onto the *same* lower dimensional space, we computed the low-dimensional embedding
615 on a "stacked" matrix created by vertically concatenating the events-by-topics topic proportions
616 matrices for the video and all 17 participants' recalls. We then divided the rows of the result (a
617 total-number-of-events by two matrix) back into separate matrices for the video topic trajectory
618 and the trajectories for each participant's recalls (Fig. 5). This general approach for discovering
619 a shared low-dimensional embedding for a collections of high-dimensional observations follows
620 Heusser et al. (2018b).

621 **Estimating the consistency of flow through topic space across participants**

622 In Figure 5B, we present an analysis aimed at characterizing locations in topic space that dif-
623 ferent participants move through in a consistent way (via their recall topic trajectories). The
624 two-dimensional topic space used in our visualizations (Fig. 5) comprised a 9x9 (arbitrary units)
625 square. We divided this space into a grid of vertices spaced 0.25 units apart. For each vertex, we
626 examined the set of line segments formed by connecting each pair successively recalled events,
627 across all participants, that passed within 0.5 units. We computed the distribution of angles formed
628 by those segments and the x -axis, and used a Rayleigh test to determine whether the distribution
629 of angles was reliably "peaked" (i.e., consistent across all transitions that passed through that local
630 portion of topic space). To create Figure 5B we drew an arrow originating from each grid vertex,
631 pointing in the direction of the average angle formed by line segments that passed within 0.5 units.
632 We set the arrow lengths to be inversely proportional to the p -values of the Rayleigh tests at each
633 vertex. Specifically, for each vertex we converted all of the angles of segments that passed within
634 0.5 units to unit vectors, and we set the arrow lengths at each vertex proportional to the length

635 of the (circular) mean vector. We also indicated any significant results ($p < 0.05$, corrected using
636 the Benjamini-Hochberg procedure) by coloring the arrows in blue (darker blue denotes a lower
637 p -value, i.e., a longer mean vector); all tests with $p \geq 0.05$ are displayed in gray and given a lower
638 opacity value.

639 **Searchlight fMRI analyses**

640 In Figure 7, we present two analyses aimed at identifying brain structures whose responses (as
641 participants viewed the video) exhibited particular temporal correlations. We developed a search-
642 light analysis whereby we constructed a cube centered on each voxel (radius: 5 voxels). For each
643 of these cubes, we computed the temporal correlation matrix of the voxel responses during video
644 viewing. Specifically, for each of the 1976 volumes collected during video viewing, we correlated
645 the activity patterns in the given cube with the activity patterns (in the same cube) collected during
646 every other timepoint. This yielded a 1976 by 1976 correlation matrix for each cube.

647 Next, we constructed two sets of “template” matrices: one reflecting the video’s topic trajectory
648 and the other reflecting each participant’s recall topic trajectory. To construct the video template, we
649 computed the correlations between the topic proportions estimated for every pair of TRs (prior to
650 segmenting the trajectory into discrete events; i.e., the correlation matrix shown in Figs. 2B and 7A).
651 We constructed similar temporal correlation matrices for each participant’s recall topic trajectory
652 (Figs. 2D, S4). However, to correct for length differences and potential non-linear transformations
653 between viewing time and recall time, we first used dynamic time warping (Berndt and Clifford,
654 1994) to temporally align participants’ recall topic trajectories with the video topic trajectory (an
655 example correlation matrix before and after warping is shown in Fig. 7B). This yielded a 1976 by
656 1976 correlation matrix for the video template and for each participant’s recall template.

657 To determine which (cubes of) voxel responses reliably matched the video template, we cor-
658 related the upper triangle of the voxel correlation matrix for each cube with the upper triangle
659 of the video template matrix (Kriegeskorte et al., 2008). This yielded, for each participant, a
660 single correlation value. We computed the average (Fisher z -transformed) correlation coefficient
661 across participants. We used a permutation-based procedure to assess significance, whereby we

662 re-computed the average correlations for each of 100 “null” video templates (constructed by circu-
663 larly shifting the template by a random number of timepoints). (For each permutation, the same
664 shift was used for all participants.) We then estimated a p -value by computing the proportion of
665 shifted correlations that were larger than the observed (unshifted) correlation. To create the map
666 in Figure 7A we thresholded out any voxels whose correlation values fell below the 95th percentile
667 of the permutation-derived null distribution.

668 We used a similar procedure to identify which voxels’ responses reflected the recall templates.
669 For each participant, we correlated the upper triangle of the correlation matrix for each cube of
670 voxels with their (time warped) recall correlation matrix. As in the video template analysis this
671 yielded a single correlation coefficient for each participant. However, whereas the video analysis
672 compared every participant’s responses to the same template, here the recall templates were
673 unique for each participant. We computed the average z-transformed correlation coefficient across
674 participants, and used the same permutation procedure we developed for the video responses to
675 assess significant correlations. To create the map in Figure 7B we thresholded out any voxels whose
676 correlation values fell below the 95th percentile of the permutation-derived null distribution.

677 References

- 678 Atkinson, R. C. and Shiffrin, R. M. (1968). Human memory: A proposed system and its control
679 processes. In Spence, K. W. and Spence, J. T., editors, *The psychology of learning and motivation*,
680 volume 2, pages 89–105. Academic Press, New York.
- 681 Baldassano, C., Chen, J., Zadbood, A., Pillow, J. W., Hasson, U., and Norman, K. A. (2017).
682 Discovering event structure in continuous narrative perception and memory. *Neuron*, 95(3):709–
683 721.
- 684 Berndt, D. J. and Clifford, J. (1994). Using dynamic time warping to find patterns in time series. In
685 *KDD workshop*, volume 10, pages 359–370.

- 686 Blei, D. M. and Lafferty, J. D. (2006). Dynamic topic models. In *Proceedings of the 23rd International*
687 *Conference on Machine Learning*, ICML '06, pages 113–120, New York, NY, US. ACM.
- 688 Blei, D. M., Ng, A. Y., and Jordan, M. I. (2003). Latent dirichlet allocation. *Journal of Machine*
689 *Learning Research*, 3:993 – 1022.
- 690 Brunec, I. K., Moscovitch, M. M., and Barense, M. D. (2018). Boundaries shape cognitive represen-
691 tations of spaces and events. *Trends in Cognitive Sciences*, 22(7):637–650.
- 692 Bylinskii, Z., Isola, P., Bainbridge, C., Torralba, A., and Oliva, A. (2015). Intrinsic and extrinsic
693 effects on image memorability. *Vision Research*, 116:165–178.
- 694 Capota, M., Turek, J., Chen, P.-H., Zhu, X., Manning, J. R., Sundaram, N., Keller, B., Wang, Y., and
695 Shin, Y. S. (2017). Brain imaging analysis kit.
- 696 Cer, D., Yang, Y., y Kong, S., Hua, N., Limtiaco, N., John, R. S., Constant, N., Guajardo-Cespedes,
697 M., Yuan, S., Tar, C., Sung, Y.-H., Strope, B., and Kurzweil, R. (2018). Universal sentence encoder.
698 *arXiv*, 1803.11175.
- 699 Chen, J., Leong, Y. C., Honey, C. J., Yong, C. H., Norman, K. A., and Hasson, U. (2017). Shared
700 memories reveal shared structure in neural activity across individuals. *Nature Neuroscience*,
701 20(1):115.
- 702 Chun, M. and Turk-Browne, N. (2007). Interactions between attention and memory. *Current opinion*
703 *in neurobiology*, 17(2):177–184.
- 704 Clewett, D. and Davachi, L. (2017). The ebb and flow of experience determines the temporal
705 structure of memory. *Curr Opin Behav Sci*, 17:186–193.
- 706 Davachi, L. (2006). Item, context and relational episodic encoding in humans. *Current Opinion in*
707 *Neurobiology*, 16(6):693—700.
- 708 Davachi, L., Mitchell, J. P., and Wagner, A. D. (2003). Multiple routes to memory: distinct medial
709 temporal lobe processes build item and source memories. *Proceedings of the National Academy of*
710 *Sciences, USA*, 100(4):2157 – 2162.

- 711 Diana, R. A., Yonelinas, A. P., and Ranganath, C. (2007). Imaging recollection and famil-
712 iarity in the medial temporal lobe: a three-component model. *Trends in Cognitive Sciences*,
713 doi:10.1016/j.tics.2007.08.001.
- 714 DuBrow, S. and Davachi, L. (2013). The influence of contextual boundaries on memory for the
715 sequential order of events. *Journal of Experimental Psychology: General*, 142(4):1277–1286.
- 716 Ezzyat, Y. and Davachi, L. (2011). What constitutes an episode in episodic memory? *Psychological
717 Science*, 22(2):243–252.
- 718 Friendly, M., Franklin, P. E., Hoffman, D., and Rubin, D. C. (1982). The Toronto Word Pool:
719 Norms for imagery, concreteness, orthographic variables, and grammatical usage for 1,080
720 words. *Behavior Research Methods and Instrumentation*, 14:375–399.
- 721 Gilboa, A. and Marlatte, H. (2017). Neurobiology of schemas and schema-mediated memory.
722 *Trends Cogn Sci*, 21(8):618–631.
- 723 Heusser, A. C., Ezzyat, Y., Shiff, I., and Davachi, L. (2018a). Perceptual boundaries cause mnemonic
724 trade-offs between local boundary processing and across-trial associative binding. *Journal of
725 Experimental Psychology Learning, Memory, and Cognition*, 44(7):1075–1090.
- 726 Heusser, A. C., Fitzpatrick, P. C., Field, C. E., Ziman, K., and Manning, J. R. (2017). Quail: a
727 Python toolbox for analyzing and plotting free recall data. *The Journal of Open Source Software*,
728 10.21105/joss.00424.
- 729 Heusser, A. C., Ziman, K., Owen, L. L. W., and Manning, J. R. (2018b). HyperTools: a Python
730 toolbox for gaining geometric insights into high-dimensional data. *Journal of Machine Learning
731 Research*, 18(152):1–6.
- 732 Howard, M. W. and Kahana, M. J. (2002). A distributed representation of temporal context. *Journal
733 of Mathematical Psychology*, 46:269–299.
- 734 Howard, M. W., MacDonald, C. J., Tiganj, Z., Shankar, K. H., Du, Q., Hasselmo, M. E., and H., E.

- 735 (2014). A unified mathematical framework for coding time, space, and sequences in the medial
736 temporal lobe. *Journal of Neuroscience*, 34(13):4692–4707.
- 737 Howard, M. W., Viskontas, I. V., Shankar, K. H., and Fried, I. (2012). Ensembles of human MTL
738 neurons “jump back in time” in response to a repeated stimulus. *Hippocampus*, 22:1833–1847.
- 739 Huk, A., Bonnen, K., and He, B. J. (2018). Beyond trial-based paradigms: continuous behavior, on-
740 going neural activity, and naturalistic stimuli. *Journal of Neuroscience*, 10.1523/JNEUROSCI.1920-
741 17.2018.
- 742 Kahana, M. J. (1996). Associative retrieval processes in free recall. *Memory & Cognition*, 24:103–109.
- 743 Koriat, A. and Goldsmith, M. (1994). Memory in naturalistic and laboratory contexts: distin-
744 guishing accuracy-oriented and quantity-oriented approaches to memory assessment. *Journal of*
745 *Experimental Psychology: General*, 123(3):297–315.
- 746 Kriegeskorte, N., Mur, M., and Bandettini, P. (2008). Representational similarity analysis – con-
747 nnecting the branches of systems neuroscience. *Frontiers in Systems Neuroscience*, 2:1 – 28.
- 748 Landauer, T. K., Foltz, P. W., and Laham, D. (1998). Introduction to latent semantic analysis.
749 *Discourse Processes*, 25:259–284.
- 750 Lerner, Y., Honey, C. J., Silbert, L. J., and Hasson, U. (2011). Topographic mapping of a hierarchy
751 of temporal receptive windows using a narrated story. *Journal of Neuroscience*, 31(8):2906–2915.
- 752 Manning, J. R. (2019). Episodic memory: mental time travel or a quantum ‘memory wave’ function?
753 *PsyArXiv*, doi:10.31234/osf.io/6zjwb.
- 754 Manning, J. R., Norman, K. A., and Kahana, M. J. (2015). The role of context in episodic memory.
755 In Gazzaniga, M., editor, *The Cognitive Neurosciences, Fifth edition*, pages 557–566. MIT Press.
- 756 Manning, J. R., Polyn, S. M., Baltuch, G., Litt, B., and Kahana, M. J. (2011). Oscillatory patterns
757 in temporal lobe reveal context reinstatement during memory search. *Proceedings of the National*
758 *Academy of Sciences, USA*, 108(31):12893–12897.

- 759 McInnes, L. and Healy, J. (2018). UMAP: Uniform manifold approximation and projection for
760 dimension reduction. *arXiv*, 1802(03426).
- 761 Mikolov, T., Chen, K., Corrado, G., and Dean, J. (2013). Efficient estimation of word representations
762 in vector space. *arXiv*, 1301.3781.
- 763 Mueller, A., Fillion-Robin, J.-C., Boidol, R., Tian, F., Nechifor, P., yoonsubKim, Peter, Rampin, R.,
764 Corvellec, M., Medina, J., Dai, Y., Petrushev, B., Langner, K. M., Hong, Alessio, Ozsvald, I.,
765 vkolmakov, Jones, T., Bailey, E., Rho, V., IgorAPM, Roy, D., May, C., foobuzz, Piyush, Seong,
766 L. K., Goey, J. V., Smith, J. S., Gus, and Mai, F. (2018). WordCloud 1.5.0: a little word cloud
767 generator in Python. *Zenodo*, <https://zenodo.org/record/1322068#.W4tPKZNKh24>.
- 768 Murdock, B. B. (1962). The serial position effect of free recall. *Journal of Experimental Psychology*,
769 64:482–488.
- 770 Paller, K. A. and Wagner, A. D. (2002). Observing the transformation of experience into memory.
771 *Trends in Cognitive Sciences*, 6(2):93–102.
- 772 Pedregosa, F., Varoquaux, G., Gramfort, A., Michel, V., Thirion, B., Grisel, O., Blondel, M., Pretten-
773 hofer, P., Weiss, R., Dubourg, V., Vanderplas, J., Passos, A., Cournapeau, D., Brucher, M., Perrot,
774 M., and Duchesnay, E. (2011). Scikit-learn: Machine learning in Python. *Journal of Machine
775 Learning Research*, 12:2825–2830.
- 776 Polyn, S. M., Norman, K. A., and Kahana, M. J. (2009). A context maintenance and retrieval model
777 of organizational processes in free recall. *Psychological Review*, 116(1):129–156.
- 778 Postman, L. and Phillips, L. W. (1965). Short-term temporal changes in free recall. *Quarterly Journal
779 of Experimental Psychology*, 17:132–138.
- 780 Rabiner, L. (1989). A tutorial on Hidden Markov Models and selected applications in speech
781 recognition. *Proceedings of the IEEE*, 77(2):257–286.
- 782 Radvansky, G. A. and Zacks, J. M. (2017). Event boundaries in memory and cognition. *Curr Opin
783 Behav Sci*, 17:133–140.

- 784 Ranganath, C., Cohen, M. X., Dam, C., and D'Esposito, M. (2004). Inferior temporal, prefrontal,
785 and hippocampal contributions to visual working memory maintenance and associative memory
786 retrieval. *Journal of Neuroscience*, 24(16):3917–3925.
- 787 Ranganath, C. and Ritchey, M. (2012). Two cortical systems for memory-guided behavior. *Nature
788 Reviews Neuroscience*, 13:713 – 726.
- 789 Schlichting, M. L. and Preston, A. R. (2015). Memory integration: neural mechanisms and impli-
790 cations for behavior. *Current Opinion in Behavioral Sciences*, 1:1–8.
- 791 Simony, E., Honey, C. J., Chen, J., and Hasson, U. (2016). Uncovering stimulus-locked network
792 dynamics during narrative comprehension. *Nature Communications*, 7(12141):1–13.
- 793 Spalding, K. N., Schlichting, M. L., Zeithamova, D., Preston, A. R., Tranel, D., Duff, M. C., and
794 Warren, D. E. (2018). Ventromedial prefrontal cortex is necessary for normal associative inference
795 and memory integration. *The Journal of Neuroscience*, 38(15):3767–3775.
- 796 Stark, S. M., Yassa, M. A., and Stark, C. E. L. (2010). Individual differences in spatial pattern
797 separation performance associated with healthy aging in humans. *Learning & Memory*, 17(6):284–
798 288.
- 799 Steyvers, M., Shiffrin, R. M., and Nelson, D. L. (2004). Word association spaces for predicting
800 semantic similarity effects in episodic memory. In Healy, A. F., editor, *Cognitive Psychology and
801 its Applications: Festschrift in Honor of Lyle Bourne, Walter Kintsch, and Thomas Landauer*. American
802 Psychological Association, Washington, DC.
- 803 Tompry, A. and Davachi, L. (2017). Consolidation promotes the emergence of representational
804 overlap in the hippocampus and medial prefrontal cortex. *Neuron*, 96(1):228–241.
- 805 Tyng, C. M., Amin, H. U., Saad, M. N. M., and S, M. A. (2017). The influences of emotion on
806 learning and memory. *Frontiers in psychology*, 8:1454.
- 807 van Kesteren, M. T. R., Beul, S. F., Takashima, A., Henson, R. N., Ruiter, D. J., and Fernández, G.

- 808 (2013). Differential roles for medial prefrontal and medial temporal cortices in schema-dependent
809 encoding: from congruent to incongruent. *Neuropsychologia*, 51(12):2352–2359.
- 810 van Kesteren, M. T. R., Ruiter, D. J., Fernández, G., and Henson, R. N. (2012). How schema and
811 novelty augment memory formation. *Trends Neurosci*, 35(4):211–9.
- 812 Waskom, M., Botvinnik, O., Okane, D., Hobson, P., David, Halchenko, Y., Lukauskas, S., Cole, J. B.,
813 Warmenhoven, J., de Ruiter, J., Hoyer, S., Vanderplas, J., Villalba, S., Kunter, G., Quintero, E.,
814 Martin, M., Miles, A., Meyer, K., Augspurger, T., Yarkoni, T., Bachant, P., Williams, M., Evans,
815 C., Fitzgerald, C., Brian, Wehner, D., Hitz, G., Ziegler, E., Qalieh, A., and Lee, A. (2016). Seaborn:
816 v0.7.1.
- 817 Welch, G. B. and Burnett, C. T. (1924). Is primacy a factor in association-formation. *American Journal
818 of Psychology*, 35:396–401.
- 819 Wiltgen, B. J. and Silva, A. J. (2007). Memory for context becomes less specific with time. *Learning
820 & Memory*, 14(4):313–317.
- 821 Yassa, M. A., Lacy, J. W., Stark, S. M., Albert, M. S., Gallagher, M., and Stark, C. E. L. (2011). Pattern
822 separation deficits associated with increased hippocampal ca3 and dentate gyrus activity in
823 nondemented older adults. *Hippocampus*, 21(9):968–979.
- 824 Yassa, M. A. and Stark, C. E. L. (2011). Pattern separation in the hippocampus. *Trends In Neuro-
825 sciences*, 34(10):515–525.
- 826 Yonelinas, A. P. (2002). The nature of recollection and familiarity: A review of 30 years of research.
827 *Journal of Memory and Language*, 46:441–517.
- 828 Zacks, J. M., Speer, N. K., Swallow, K. M., Braver, T. S., and Reynolds, J. R. (2007). Event perception:
829 a mind-brain perspective. *Psychological Bulletin*, 133:273–293.
- 830 Zadbood, A., Chen, J., Leong, Y. C., Norman, K. A., and Hasson, U. (2017). How we transmit
831 memories to other brains: Constructing shared neural representations via communication. *Cereb
832 Cortex*, 27(10):4988–5000.

833 Zwaan, R. A. and Radvansky, G. A. (1998). Situation models in language comprehension and
834 memory. *Psychological Bulletin*, 123(2):162 – 185.

835 **Supporting information**

836 Supporting information is available in the online version of the paper.

837 **Acknowledgements**

838 We thank Luke Chang, Janice Chen, Chris Honey, Lucy Owen, Emily Whitaker, and Kirsten Ziman
839 for feedback and scientific discussions. We also thank Janice Chen, Yuan Chang Leong, Kenneth
840 Norman, and Uri Hasson for sharing the data used in our study. Our work was supported in part
841 by NSF EPSCoR Award Number 1632738. The content is solely the responsibility of the authors
842 and does not necessarily represent the official views of our supporting organizations.

843 **Author contributions**

844 Conceptualization: A.C.H. and J.R.M.; Methodology: A.C.H. and J.R.M.; Software: A.C.H., P.C.F.
845 and J.R.M.; Analysis: A.C.H., P.C.F. and J.R.M.; Writing, Reviewing, and Editing: A.C.H., P.C.F.
846 and J.R.M.; Supervision: J.R.M.

847 **Author information**

848 The authors declare no competing financial interests. Correspondence and requests for materials
849 should be addressed to J.R.M. (jeremy.r.manning@dartmouth.edu).